

Quantum mechanical and RRKM studies of the reactions $\text{CH}_3 + \text{ClO} \rightarrow \text{CH}_3\text{O} + \text{Cl}$ and $\text{CH}_3\text{O} + \text{Cl} \rightarrow \text{HCHO} + \text{HCl}$

E. Drougas, D.K. Papayannis, A.M. Kosmas*

Department of Chemistry, Physical Chemistry Laboratory, University of Ioannina, Ioannina 45110, Greece

Received 7 May 2001

Abstract

Bimolecular rate coefficients based on variational RRKM theory are calculated for the reaction of methyl radicals with chlorine monoxide and the reaction of methoxy radicals with chlorine atoms. The reaction pathways, established by ab initio calculations, are found to involve the intermediate formation of methyl hypochlorite. Our computations agree well with recent ab initio data on CH_3OCl thermal decomposition channels and also the resulting rate coefficients are found in good agreement with the experimental measurements. © 2002 Elsevier Science B.V. All rights reserved.

1. Introduction

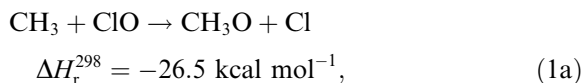
The important role of Cl atoms and ClO radicals in the rapid depletion of stratospheric ozone over Antarctica [1,2] has given the opportunity for the investigation of the reactions of these species with several radicals of atmospheric significance. An interesting such system is the reaction of chlorine monoxide with methyl radicals [3]



Although not directly associated with the stratospheric ozone chemistry, it is worthy of study, being essential for kinetic and mechanistic information on the reaction



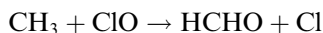
which is an important process in ozone depletion cycles [3–7]. In addition, reaction (1) is an interesting system from the theoretical point of view, resembling the $\text{CH}_3 + \text{OH}$ kinetics [8,9] and being the methyl analogue of the well-studied $\text{H} (^2\text{S}) + \text{ClO} (^2\Pi)$ reaction [10], relevant also to $\text{O} (^3\text{P}) + \text{HCl} (^1\Sigma^+)$ [11] and $\text{HO} + \text{Cl}$ systems [12,13]. Experimentally, it has been investigated by Wayne and coworkers [3] who found that it is a very fast process with a rate constant $k = (1.3 \pm 0.4) \times 10^{-10} \text{ cm}^3 \text{ molecule}^{-1} \text{ s}^{-1}$ at 298 K and with the major channel being the formation of methoxy radicals and chlorine atoms



A four-center elimination process may be also considered in principle, according to the following scheme:

* Corresponding author. Fax: +30-5109-8798.

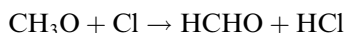
E-mail address: amyloa@cc.uoi.gr (A.M. Kosmas).



$$\Delta H_r^{298} = -106.8 \text{ kcal mol}^{-1} \quad (1b)$$

To the best of our knowledge there has been no experimental evidence that any other products are formed except those of reaction (1a) nor of any pressure dependence of the rate coefficient. Therefore, from the experimental studies it has been concluded that the reaction proceeds directly to form $\text{CH}_3\text{O} + \text{Cl}$, consisting this way a good method of producing methoxy radicals for very specialized studies [14,15]. It is quite possible however, that the experimental difficulties have obscured the detection of channel (1b).

The molecular elimination reaction



$$\Delta H_r^{298} = -81.3 \text{ kcal mol}^{-1} \quad (2)$$

is also an interesting related system. Methoxy radicals are important intermediates in the oxidation mechanism of the hydrocarbons either in combustion systems or in atmospheric processes. The experimental measurements [16,17] have established $\text{HCHO} + \text{HCl}$ as the main products. However, a large ambiguity of an order of magnitude exists in the value of the rate coefficient at 298 K. Two results have been reported in the literature, $k = (1.0 \pm 0.2) \times 10^{-10} \text{ cm}^3 \text{ molecule}^{-1} \text{ s}^{-1}$ [16] and $k = (1.9 \pm 0.4) \times 10^{-11} \text{ cm}^3 \text{ molecule}^{-1} \text{ s}^{-1}$ [17] and thus, it would be useful to have a theoretical investigation too.

In the present work we carry out a theoretical investigation of reactions (1) and (2). The stationary points and the reaction pathways for the initial association steps are established in each case by ab initio calculations at the MP2(full)/6-31++G(3df, 3dp) level of theory. The stationary points are additionally investigated at the CCSD(T)/6-31++G(3df, 3dp) level of theory at the MP2(full)/6-31++G(3df, 3dp) optimized geometries. Both title reactions are found to involve the intermediate formation of methyl hypochlorite and its subsequent decomposition to various products. From this point of view our calculations are in excellent agreement with recent calculations on CH_3OCl thermal decomposition channels [18]. Next, bimolecular rate coefficients at 298 K are

calculated for the title reactions using variational RRKM theory [19–22] on a number of points along the initial addition step for each reaction. The results are found in very good agreement with the available experimental data.

2. Quantum mechanical calculations and results

The geometries of all reactants, products and stationary points have been fully optimized at the MP2(full)/6-31++G(3df, 3dp) level of theory. Partition functions, moments of inertia and harmonic vibrational frequencies were calculated at the same level of theory and have been used for the characterization of the stationary points, the zero-point energy (ZPE) corrections and the RRKM computations. To obtain reliable energy differences we also carried out single-point CCSD(T)/6-31++G(3df, 3dp) calculations at the MP2(full)/6-31++G(3df, 3dp) optimized geometries and the so computed energy differences have been used for the RRKM applications. No energy barriers have been found at the entrance of either reaction and so the first step in each of these processes involves the barrierless association of the reactants. Fol-

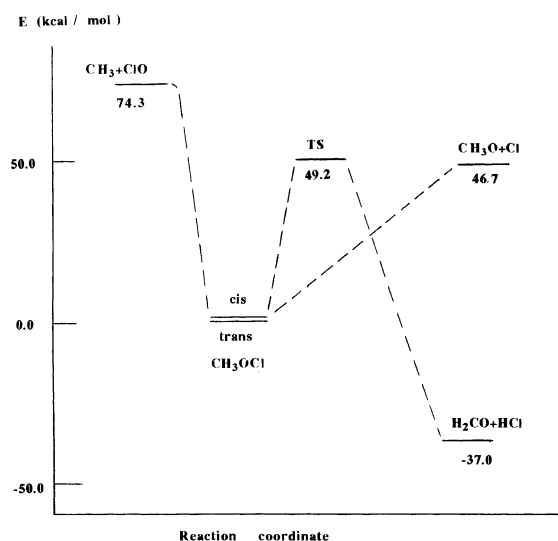


Fig. 1. Potential energy profiles for the reactions $\text{CH}_3 + \text{ClO} \rightarrow \text{products}$ (1) and $\text{CH}_3\text{O} + \text{Cl} \rightarrow \text{HCHO} + \text{HCl}$ (2).

lowing the procedure adopted by Schatz and coworkers [22] in the study of the reactions of C, CH and $^1\text{CH}_2$ species with acetylene, several points at the entrance pathway of each reaction have been examined, also at the MP2(full)/6-31++G(3df,3pd) level of theory to allow a variational evaluation of the rate coefficient. On the basis of these results the reaction energy profiles, confirmed by IRC calculations, have been computed and they are depicted in Fig. 1. All calculations were performed using the GAUSSIAN 98 series of programs [23]. The geometrical parameters, harmonic frequencies and moments of inertia of reactants, products and stationary points are summarized in Table 1 and their relative energetics is given in Table 2.

As already mentioned, both reactions are found to proceed through barrierless association pathways to the intermediate formation of energized methyl hypochlorite, CH_3OCl in the *trans* – minimum energy configuration. CH_3OCl is a well studied compound both experimentally [24–26] and theoretically [27–32]. A transition state (TS) has been also determined in the pathway that leads to the elimination channel $\text{HCHO} + \text{HCl}$, located at $2.6 \text{ kcal mol}^{-1}$ above $\text{CH}_3\text{O} + \text{Cl}$. In reaction (1a) the energized bound intermediate CH_3OCl suffers a O–Cl bond scission and produces methoxy radicals and Cl atoms. The O–Cl bond distance increases from 1.544 \AA in reactant ClO to 1.677 \AA in the minimum energy *trans*- CH_3OCl and increases further until it breaks completely and the

Table 1

Structural parameters^a and harmonic frequencies^b for reactants, products and stationary points and moments of inertia^c for stationary points for the title reactions at the MP2/ 6-31++G(3df,3pd) level of theory

Species	CH_3OCl	<i>cis</i> - CH_3OCl	ClOCH_3HCl	CH_3O	HCHO	TS^d	
$r(\text{CO})$	1.421	1.432		1.368	1.209	1.293	1.304 ^d
$r(\text{OCl})$	1.677	1.674	1.544			2.280	2.343
$r(\text{H}^1\text{C})$	1.083	1.081	1.071	1.094		1.242	1.231
$r(\text{H}^2\text{C})$	1.085	1.084	1.071	1.087	1.095	1.096	1.096
$r(\text{H}^3\text{C})$	1.085	1.084	1.071	1.087	1.095	1.096	1.096
$r(\text{HCl})$			1.261				
$\angle \text{COCl}$	109.7	112.3				92.9	91.2
$\angle \text{H}^1\text{CO}$	104.4	111.6		105.2		97.5	97.7
$\angle \text{H}^2\text{CO}$	111.1	108.1		112.8	121.8	117.3	
$\angle \text{H}^3\text{CO}$	111.1	108.1		112.8	121.8	117.3	
H^1COCl	180.0	0.0				0.0	0.0
Frequencies							
CH_3OCl^d	3235, 3203, 3111, 1538, 1504, 1479, 1211, 1193, 1059, 720, 373, 257 3031 ^d , 3001, 2910, 1457, 1421, 1398, 1131, 1112, 989, 654, 347, 232						
<i>cis</i> - CH_3OCl	3241, 3222, 3125, 1532, 1514, 1487, 1209, 1172, 1051, 714, 409, 251i 3028, 3022, 2922, 1448, 1400, 1126, 1080, 985, 651, 379, 264i ^d						
CH_3	3385, 3206, 1436, 376						
OCl	862						
HCl	3131						
CH_3O	3178, 3134, 3050, 1552, 1441, 1424, 1145, 981, 806						
HCHO	3091, 3023, 1777, 1558, 1284, 1199						
TS^d	3133, 3029, 1669, 1523, 1302, 1247, 1150, 940, 524, 411, 361, 3087i 2937 ^d , 2843, 1564, 1458, 1223, 1163, 1121, 948, 487, 377, 311, 2869i						
	I_a	I_b	I_c	I_r			
CH_3OCl	47.0	330.2	365.6	5.0			
TS	55.0	351.1	393.5	5.7			

^a In \AA and degrees.

^b In cm^{-1} .

^c In amu \AA^2 .

^d The column and the row labeled d contain the corresponding results of [18].

Table 2

Total and relative energies for various species involved in the $\text{CH}_3 + \text{ClO}$ and $\text{CH}_3\text{O} + \text{Cl}$ reactions

Species	CCSD(T) ^a	MP2 ^a	ZPE ^b	ΔE^c	$\Delta_r H_{298}^d$
$\text{CH}_3 + \text{ClO}$	−574.49371	−574.42201	20.1	0.0	0.0
CH_3OCl (min)	−574.62324	−574.56831	27.0	−74.4	−84.9
CH_3OCl (<i>cis</i>)	−574.61846	−574.56329	26.7	−71.7	−81.8
$\text{CH}_3\text{O} + \text{Cl}$	−574.54382	−574.47553	23.9	−27.6	−29.8
TS	−574.53625	−574.46485	21.8	−25.0	−25.2
$\text{HCHO} + \text{HCl}$	−574.67279	−574.61945	21.5	−111.0	−122.5
					−106.8

^a Electronic energies in Hartrees.^b ZPE in kcal mol^{-1} .^c ΔE in kcal mol^{-1} are the energy differences including ZPE energies with respect to $\text{CH}_3 + \text{ClO}$, first column based on the CCSD(T) results and second column on the MP2 calculations, respectively.^d The enthalpies of reaction at 298 K given in [1].

products $\text{CH}_3\text{O} + \text{Cl}$ are formed. It is apparent that the energy of the reactants deposited in energized CH_3OCl , is mainly directed into the O–Cl bond which eventually dissociates. The products $\text{CH}_3\text{O} + \text{Cl}$ are formed at an energy height $46.7 \text{ kcal mol}^{-1}$ with respect to minimum energy CH_3OCl and $27.6 \text{ kcal mol}^{-1}$ below the reactants $\text{CH}_3 + \text{ClO}$. There is another possibility, however, for the CH_3OCl intermediate to follow. It may proceed through the tight four-center TS to produce the elimination products $\text{HCHO} + \text{HCl}$, as it will be described next for the reaction pathway between methoxy radicals and Cl atoms. Since the TS is placed at $2.6 \text{ kcal mol}^{-1}$ above $\text{CH}_3\text{O} + \text{Cl}$ this competing elimination pathway (1b) is expected to be less important than the barrierless O–Cl bond scission (1a), in consistency with the experimental observations which indicate channel (1a) as the major channel of reaction (1). Nevertheless, it cannot be ignored and must be taken into account in the computation of the rate coefficient.

In reaction (2) the reagents CH_3O and Cl being at a lower energy level than the reactants in reaction (1), form again the bound CH_3OCl intermediate through a barrierless association step. The minimum energy *trans*- CH_3OCl proceeds to the planar *cis*-configuration where the H^1 atom approaches the Cl atom. The C– H^1 and Cl–O distances in *trans*- CH_3OCl , 1.083 and 1.677 Å, respectively, and the O–C– H^1 and the Cl–O–C bond angles, 104.5° and 109.7° , respectively, change to 1.081, 1.674 Å, and 111.6° , 112.3° , respectively, in the *cis*-configuration and the Cl–O–

C– H^1 dihedral angle changes from 180° to 0° . Thus, the Cl and H^1 atoms approach each other and their distance decreases to 2.558 Å. The system further proceeds through the tight TS where the H^1 –Cl distance decreases further to 1.891 Å and the H^1 –C and O–Cl distances increase to 1.242 and 2.280 Å, respectively, from the *cis*-configuration, while the H^1CO and COCl bond angles decrease to 97.5° and 92.9° . All four atoms H^1 , C, O and Cl keep in a plane during the whole process. The TS presents a C_s symmetry with a tight, four-member ring structure and presents an imaginary frequency, 3087 cm^{-1} , which compares very well with the value 2869 cm^{-1} of the corresponding structure in [18]. Gradually the H^1C and OCl bonds are further elongated, the H^1 migrates to the Cl atom and eventually HCl and HCHO are formed. The energy barrier where the TS is located for this 1, 2 elimination process is calculated to be $2.6 \text{ kcal mol}^{-1}$ above $\text{CH}_3\text{O} + \text{Cl}$ reactants.

Since the initial addition steps for both reactions are barrierless, it is essential to ascertain detailed information about these steps for the proper evaluation of the rate coefficients. To this purpose, we determined energies, frequencies and moments of inertia at points along the entrance of the minimum energy path for the initial addition step of each of reactions (1) and (2). The calculations are carried out by fixing the reaction coordinate, $r(\text{C–O})$ and $r(\text{O–Cl})$, respectively, and allow full optimization of the remaining structural parameters. The data for these points, labeled p1a to p1f and p2a to p2f for each reaction are collected in Tables 3 and 4.

Table 3

Energies, frequencies, moments of inertia and resulting rate coefficients along the entrance channel for $\text{CH}_3 + \text{ClO}$ reaction

Energy (kcal/mol)	p1a −4.6	p1b −1.9	p1c −1.5	p1d −1.2	p1e −0.5	p1f −0.2
Harmonic frequencies (cm^{-1})	3352 3351 3159 1463 1462 1013 782 607 570 216 70 272i	3354 3353 3160 1464 1463 996 786 593 555 212 66 273i	3354 3353 3160 1464 1463 992 787 589 552 210 65 273i	3354 3353 3160 1464 1463 994 786 591 554 211 65 273i	3354 3354 3161 1464 1463 987 788 586 548 210 64 273i	3354 3354 3161 1464 1463 985 788 584 547 209 64 273i
Moments of inertia ($\text{amu } \text{\AA}^2$)	20.5 119.1 136.0	21.1 121.7 134.4	20.7 121.3 135.2	21.2 122.1 135.9	20.0 124.0 139.4	20.5 124.2 141.0
$k_2(T) \times 10^{-10}$ ($\text{cm}^3 \text{ molecule}^{-1} \text{ s}^{-1}$)	1184.5	89.7	59.0	3.2	1.7	1.5
$k_3(T) \times 10^{-10}$ ($\text{cm}^3 \text{ molecule}^{-1} \text{ s}^{-1}$)	323.1	27.0	23.8	1.2	0.5	0.4

Table 4

Energies, frequencies, moments of inertia and resulting rate coefficients along the entrance channel for $\text{CH}_3\text{O} + \text{Cl}$ reaction

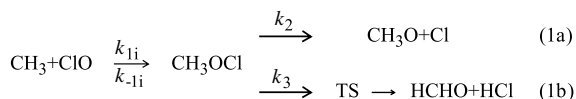
Energy (kcal/mol)	p2a −3.2	p2b −2.1	p2c −1.3	p2d −1.0	p2e −0.5	p2f −0.0
Harmonic frequencies (cm^{-1})	3106 3060 2974 1551 1447 1415 1191 1172 1015 240 228 223i	3102 3056 2969 1551 1446 1412 1191 1172 1016 236 226 226i	3099 3053 2966 1551 1445 1410 1190 1172 1017 233 224 228i	3099 3052 2965 1551 1445 1410 1190 1172 1017 232 223 228i	3097 3050 2963 1552 1444 1408 1189 1172 1017 230 222 230i	3095 3048 2961 1552 1443 1407 1189 1172 1018 228 221 230i
Moments of inertia ($\text{amu } \text{\AA}^2$)	13.9 133.2 143.1	14.0 133.4 143.9	13.5 134.1 145.3	13.6 138.1 145.9	13.9 144.8 146.7	14.2 145.2 147.0
$k'_2 \times 10^{-11}$ ($\text{cm}^3 \text{ molecule}^{-1} \text{ s}^{-1}$)	192	25	7.6	1.9	1.4	1.4

3. RRKM calculations

In this section we apply an extension of RRKM theory for the calculation of the macrocanonical bimolecular rate constants at 298 K for the title

reactions as applied in other bimolecular reactions in which an intermediate complex is formed [33–35].

(1) $\text{CH}_3 + \text{ClO}$: We first present a brief analysis for reaction (1) assuming the following scheme:



Here k_{1i} is the microcanonical rate constant for forward reaction and k_{-1i} is the microcanonical rate constant for back reaction, depending on the particular point of the entrance pathway in a way that will be explained later. The microcanonical rate constants k_2 and k_3 are the forward rate coefficients for the production of the two sets of products.

The two reactants CH_3 and ClO are assumed to have enough energy to form the products on a potential energy profile such as given in Fig. 1. The intermediate complex $\text{M} = \text{CH}_3\text{OCl}$ is formed “hot” in the low pressure limit at a well depth V_M with respect to reactants and its formation is hindered by a potential energy barrier which may be a positive quantity or zero with respect to reactants. An energy barrier hinders the decomposition of the intermediate activated complex M to products. This is just the energy barrier at which the products $\text{CH}_3\text{O} + \text{Cl}$ are located with respect to reactants for channel (1a) or the energy barrier where the TS is located with respect to reactants for channel (1b). Since CH_3OCl is a stable intermediate with respect to products, all the states are assumed quantized at the energy at which it is formed with the exception of the internal degree of freedom corresponding to the reaction coordinate which is quantized only up to the lowest channel out of the potential well. Thus, the reaction is analyzed from the point of view of the options available to the intermediate minimum and the overall reaction rate coefficient $k(T)$ includes the macrocanonical rate constants for each channel, which we denote $k_2(T)$ and $k_3(T)$, respectively, $k(T) = k_2(T) + k_3(T)$.

The microcanonical rate constant, $k_i(E, J)$, for a given reaction step at an initial reactant energy E is given by

$$k_i(E, J) = W_i(E, J)/h\varrho_M(E, J), \quad (3)$$

where $\varrho_M(E, J)$ is the density of states available to the minimum at a reactant energy E and $W_i(E, J)$

is the number of states for the active degrees of freedom of the transition state TS_i being involved in the considered reaction step $i = a, b$. Applying steady state theory to the intermediate species (*trans*- CH_3OCl) it is readily determined that the macrocanonical rate constant $k_2(T)$ for channel (1a) at 298 K, which is the quantity of interest here, is given by

$$k_2(T) = \frac{1}{hQ_{\text{CH}_3}Q_{\text{ClO}}} \sum_{J=0}^{\infty} \int \frac{W_2(E, J)e^{-E/RT}}{1 + \beta(E, J)} dE. \quad (4)$$

An analogous expression holds for channel (1b)

$$k_3(T) = \frac{1}{hQ_{\text{CH}_3}Q_{\text{ClO}}} \sum_{J=0}^{\infty} \int \frac{W_3(E, J)e^{-E/RT}}{1 + \beta(E, J)} dE, \quad (5)$$

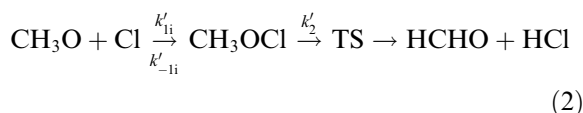
Q_{CH_3} and Q_{ClO} are the relevant partition functions and the microcanonical branching ratio $\beta(E, J)$ is given as

$$\beta(E, J) = \frac{k_2(E, J) + k_3(E, J)}{k_{-1i}(E, J)}. \quad (6)$$

To determine $k_2(T)$ and $k_3(T)$ from (4) and (5) the quantities $W_2(E, J)$, $W_3(E, J)$ and the microcanonical rate constants $k_2(E, J)$, $k_3(E, J)$ and $k_{-1i}(E, J)$ are evaluated using a modified version of the RRKM code [36] based on RRKM theory [19,20]. The required input contains in general, the moments of inertia of the intermediate minimum and the harmonic frequencies, the moments of inertia and the relative energetics of the barriers that hinder the decomposition of the minimum to either reactants or products. Also the symmetry factor is required which was given the value 3. The calculation of k_{-1i} presents complications since the reaction involves a barrierless initial addition pathway and there is no well-defined TS configuration whose molecular properties may be used in the calculation of k_{-1i} . Thus, a variational method is employed to determine k_{-1i} . According to variational theory, the bottleneck of a reaction occurs at a point along the minimum energy path where the number of states available, and hence the microcanonical rate constant, is at a minimum. This means that calculations must be done at various points along the minimum energy path until a minimum in the rate is found, thereby defining the

reactive bottleneck. For reaction (1) we calculated rate constants k_{-li} for all the ab initio points pli, $i = a \dots f$, included in Table 3. We found that the minimum in the resulting bimolecular rate constants occur at the highest energy point, as we shall see in Section 4.

(2) $\text{CH}_3\text{O} + \text{Cl}$: Reaction (2) is assumed to proceed according to the following scheme:



The macrocanonical rate coefficient $k'_2(T)$ at 298 K is calculated from

$$k'_2(T) = \frac{1}{hQ_{\text{CH}_3\text{O}}Q_{\text{Cl}}} \sum_{J=0}^{\infty} \int \frac{W'_2(E, J) e^{-E/RT}}{1 + \beta'(E, J)} dE, \quad (7)$$

where the branching ratio $\beta'(E, J)$ is given by

$$\beta'(E, J) = \frac{k'_2(E, J)}{k'_{-li}(E, J)}. \quad (8)$$

The microcanonical rate constants k'_{-li} have been calculated for all the ab initio points p2i, $i = a, \dots, f$, included in Table 4.

A final point to elucidate is the evaluation of the reduced moment of inertia, I_r . To calculate I_r of the internal rotation for the intermediate complex and the TS, the approximation found in Chemical Thermodynamics textbooks was employed [21,37–39]. For two groups rotating relative to one of the axes of the molecule, I_r is found by the equation

$$I_r = \frac{I_A I_B}{I_A + I_B}, \quad (9)$$

where I_A and I_B are the moments of inertia of the two groups rotating with respect to each other around the molecular axis.

4. Results and conclusions

The macrocanonical rate constants $k_2(T)$, $k_3(T)$ and $k'_2(T)$, calculated at 298 K by numerical evaluation of Eqs. (4), (5) and (7) vs. a series of ab initio path points are included in Tables 4 and 5 and they are also depicted in Figs. 2–4. The figures show that indeed in all systems the minimum rate constants are associated with the highest energy point in each case, i.e., the rate coefficient becomes a minimum at zero energy difference with respect to reactants. The minimum values for $k_2(T)$ and $k'_2(T)$ are compared in Table 5 to the corresponding experimental results of Wayne and coworkers [3] for reaction (1a) and of Daele et al. [17] for reaction (2). A good agreement is clearly seen, taking into account the uncertainty both in finding the minima in Fig. 2 and in the experimental measurements. The rate constant for channel (1b), $k_3(T)$, is calculated about one fourth of the value of $k_2(T)$. This means that channel (1b) plays a secondary but non-negligible

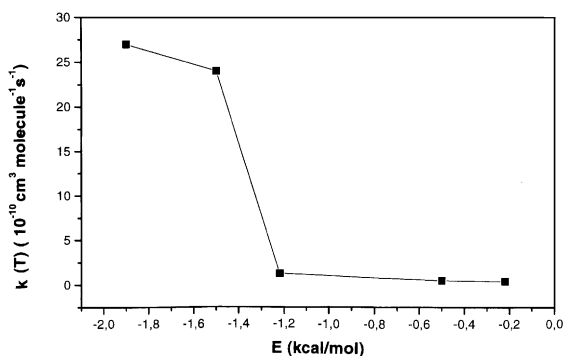


Fig. 2. Variational macrocanonical rate coefficients at 298 K vs. ab initio reaction path points for reaction (1a). The point at $-4.6 \text{ kcal mol}^{-1}$ is not included as it does not fit into the diagram.

Table 5

Best estimated rate constants in $\text{cm}^3 \text{ molecule}^{-1} \text{ s}^{-1}$ for reactions (1a) and (2) at 298 K

	$k_2(T)$	$k'_2(T)$
Theoretical	1.5×10^{-10}	1.4×10^{-11}
Experimental	$(1.3 \pm 0.4) \times 10^{-10a}$	$(1.0 \pm 0.2) \times 10^{-10a}, (1.9 \pm 0.4) \times 10^{-11b}$

^a Ref. [3].

^b Refs. [16,17].

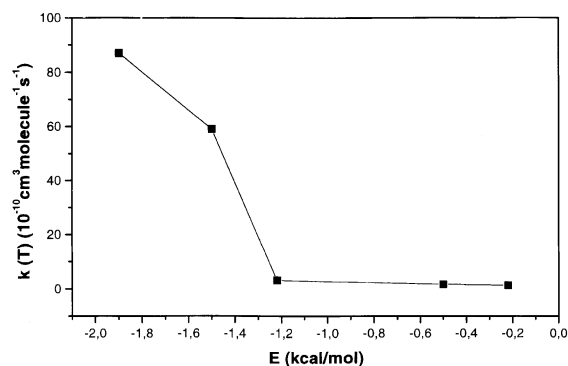


Fig. 3. Variational macrocanonical rate coefficients at 298 K vs. ab initio reaction path points for reaction (1b). The point at $-4.6 \text{ kcal mol}^{-1}$ is not included as it does not fit into the diagram.

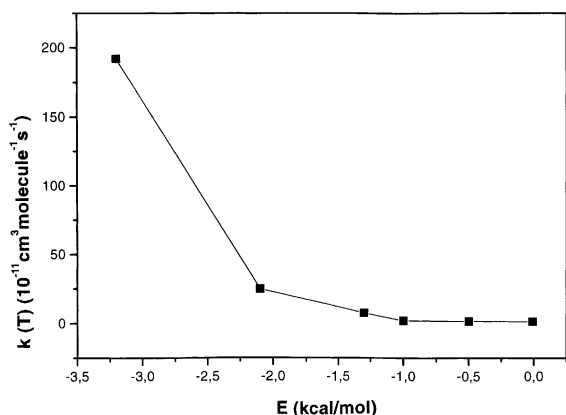


Fig. 4. Variational macrocanonical rate coefficients at 298 K vs. ab initio reaction path points for reaction (2).

role in the rate of the overall reaction between CH_3 and ClO .

To summarize, both reactions studied in the present work, namely the reactions of methyl radicals with chlorine monoxide and the reactions of methoxy radicals with chlorine atoms involve the intermediate formation of “hot” methyl hypochlorite. With a degree of activation depending on the initial energy level of the reagents the activated complex proceeds either directly to the formation of $\text{CH}_3\text{O} + \text{Cl}$ through channel (1a) or through the TS to $\text{HCHO} + \text{HCl}$, channel (1b), which plays a minor but non-negligible role in the overall rate constant $k(T)$. No significant barrier is encountered

for the decomposition of this activated intermediate into $\text{CH}_3\text{O} + \text{Cl}$ and as a result a very large rate coefficient $k_2(T) = 1.5 \times 10^{-10} \text{ cm}^3 \text{ molecule}^{-1} \text{ s}^{-1}$ is obtained, close to the collision frequency. In reaction (2) the bound intermediate formed passes through the tight TS to the elimination products $\text{HCHO} + \text{HCl}$ with a lower rate coefficient $k'_2(T) = 4.0 \times 10^{-11} \text{ cm}^3 \text{ molecule}^{-1} \text{ s}^{-1}$, still large compared to other gas-phase processes. Thus, in the second case, reaction (2), the well characterized TS, intervenes between the “hot” intermediate and the $\text{HCl} + \text{HCHO}$ products, resulting in a lower rate coefficient. Consequently, our theoretical result supports the experimental measurements of Daele et al. [17] rather than that of [16] and it is the reasonable consequence of the existence of the TS which has been verified in the path of the four-center elimination process in both [17,27] and the present work.

References

- [1] M.J. Molina, F.S. Rowland, *Nature* 249 (1974) 810.
- [2] L.T. Molina, M.J. Molina, *J. Phys. Chem.* 91 (1987) 433.
- [3] P. Piggs, C.E. Canosa-Mas, J.-M. Fracheboud, G. Marston, D.E. Shallcross, R.P. Wayne, *J. Chem. Soc. Faraday Trans.* 91 (1995) 3045.
- [4] F.G. Simon, J.P. Burrows, W. Schneider, G.K. Moortgat, P. Grutzen, *J. Phys. Chem.* 93 (1989) 7807.
- [5] W.B. DeMore, *J. Geophys. Res.* 96 (1991) 4995.
- [6] F. Helleis, J.N. Crowley, G.K. Moortgat, *J. Phys. Chem.* 97 (1993) 11464.
- [7] R.D. Kenner, K.R. Ryan, I.C. Plumb, *Geophys. Res. Lett.* 20 (1993) 1571.
- [8] L.B. Harding, H.B. Schlegel, R. Krishnan, J.A. Pople, *J. Phys. Chem.* 84 (1980) 3394.
- [9] S.P. Walch, *J. Chem. Phys.* 98 (1993) 3163.
- [10] S.J. Wategaonkar, D.W. Setser, *J. Chem. Phys.* 90 (1989) 6224, and references therein.
- [11] H. Koizumi, G.C. Schatz, M.S. Gordon, *J. Chem. Phys.* 95 (1991) 6421, and references therein.
- [12] S. Skokov, K.A. Peterson, J.M. Bowman, *J. Chem. Phys.* 109 (1998) 2662.
- [13] J. Koput, K.A. Peterson, *Chem. Phys. Lett.* 283 (1998) 139.
- [14] P. Piggs, C.E. Canosa-Mas, J.-M. Fracheboud, D.E. Shallcross, R.P. Wayne, *J. Chem. Soc. Faraday Trans.* 93 (1997) 2481.
- [15] R.P. Wayne, private communication.
- [16] T. Jung Kamp, A. Kukui, R.N. Schindler, *Ber. Bunsenges. Phys. Chem.* 99 (1995) 1057.
- [17] V. Daele, G. Laverdet, G. Poulet, *Int. J. Chem. Kinet.* 28 (1996) 589.

- [18] T.-J. He, D.-M. Chen, F.-C. Liu, L.-S. Sheng, *Chem. Phys. Lett.* 332 (2000) 545.
- [19] J.I. Steinfeld, J.S. Francisco, W.L. Hase, *Chemical Kinetics and Dynamics*, Prentice-Hall, Englewood Cliffs, NJ, 1989.
- [20] T. Baer, W.L. Hase, *Unimolecular Reaction Dynamics*, Oxford University Press, New York, 1996.
- [21] Y.-P. Liu, D.-h. Lu, A. Gonzalez-Lafont, D.G. Truhlar, B.C. Garrett, *J. Am. Chem. Soc.* 115 (1993) 7806.
- [22] R. Guadagnini, G.C. Schatz, S.P. Walch, *J. Phys. Chem. A* 102 (1998) 5857.
- [23] M.J. Frisch, et al., *GAUSSIAN 98*, Gaussian Inc., Pittsburgh, PA, 1998.
- [24] J.S. Rigden, S.S. Butcher, *J. Chem. Phys.* 40 (1964) 2109.
- [25] J.N. Crowley, F. Helleis, R. Muller, G.K. Moortat, P.J. Crutzen, J.J. Orlando, *J. Geophys. Res.* 99 (1994) 20683.
- [26] T.P.W. Jung Kamp, U. Kirchner, M. Schmidt, R.N. Schindler, *J. Photochem. Photobiol. A* 91 (1995) 1.
- [27] B.M. Messer, M.J. Elrod, *Chem. Phys. Lett.* 301 (1999) 10.
- [28] J. Espinosa-Garcia, *Chem. Phys. Lett.* 315 (1999) 239.
- [29] J.S. Francisco, *Int. J. Quantum Chem.* 73 (1999) 29.
- [30] Y. Li, J.S. Francisco, *J. Chem. Phys.* 111 (1999) 8384.
- [31] J. Espinosa-Garcia, *Chem. Phys. Lett.* 316 (2000) 563.
- [32] D. Jung, C.-J. Chen, J.W. Bozzelli, *J. Phys. Chem. A* 104 (2000) 9581.
- [33] M. Mozurkewich, S.W. Benson, *J. Phys. Chem.* 88 (1984) 6429.
- [34] Y. Chen, A. Rauk, E. Tschuikow-Roux, *J. Phys. Chem.* 95 (1991) 9900.
- [35] M. Simonson, K.S. Bradley, G.C. Schatz, *Chem. Phys. Lett.* 244 (1995) 19.
- [36] L. Zhu, W.L. Hase, *QCPE* 644.
- [37] J.G. Aston, J.J. Fritz, *Thermodynamics and Statistical Thermodynamics*, Wiley, New York, 1959.
- [38] M.Kh. Karapetyants, *Chemical Thermodynamics*, Mir Publishers, Moscow, 1978.
- [39] N. Davidson, *Statistical Mechanics*, McGraw-Hill, New York, 1962.